

Medium- and Large-Scale Characterization of UMTS-Allocated Frequency Division Duplex Channels

Sana Salous, *Member, IEEE*, and Hulya Gokalp

Abstract—A dual-band sounder is used in both trolley and van measurements in the dense urban environment of Manchester city center to characterize the uplink (1920–1980 MHz) and downlink (2110–2170 MHz) frequency-division duplex (FDD) channels allocated to third-generation (3G) mobile radio systems. The data are analyzed with 60- and 5-MHz resolutions, as used for 3G wideband code-division multiple-access systems. Root-mean-square (rms) delay spread and 15-dB widths of mainly temporally averaged delay profile are presented either as cumulative distribution functions (cdfs) for each individual frequency band or as histograms of the difference between uplink and downlink on a local area basis. It was found that the histograms show larger differences between the two bands than the individual cdf and that the differences between the FDD channels are more pronounced on circumferential routes and shadowed locations. Correlations of rms delay spread with excess path loss and distance are on the order of 0.5 and 0.4, respectively.

Index Terms—Excess path loss, frequency division duplex (FDD), root-mean-square (rms) delay spread, third generation (3G), wideband code-division multiple access (W-CDMA).

I. INTRODUCTION

WITH more demand for high data rates, the frequency bands between 1920–1980 and 2110–2170 MHz have been allocated as the uplink and downlink bands for third-generation (3G) mobile radio systems known as International Mobile Telecommunications-2000 or the Universal Mobile Telecommunications System (UMTS). These systems provide variable data rates to accommodate a wide range of services using code-division multiple access (CDMA) with 4.4- to 5.2-MHz channel spacing. In addition to soft handover and enhanced capacity, CDMA systems enable the use of RAKE receivers, which are able to resolve multipath components within

the chip rate and to combine them coherently, hence exploiting multipath diversity. To achieve this, the RAKE receiver continuously searches for multipath components with significant energy content. Since the number of resolved multipath components and their relative power are a function of the transmitted frequency and bandwidth [1], [2], it is desirable to characterize the two 60-MHz frequency bands from simultaneous measurements using a measurement technique that enables the processing of the data with different bandwidths. The comparison of adjacent 5-MHz bands and between corresponding uplink and downlink bands provides information on the possible frequency allocation for a particular user and whether the information derived from the uplink multipath structure can be used for the transmission of downlink information and vice versa. The estimation of the window over which significant multipath energy is likely to arrive helps determine the width of the search engine of the RAKE receiver.

Despite the significant number of measurement campaigns both indoor and outdoor, the different frequency band measurements tended to be performed at frequencies with considerable frequency separation [3]–[5]. Apart from the simultaneous measurements over 10-MHz bandwidth, where 195-kHz sections of the bandwidth were analyzed to determine the frequency correlation function of the channel for Global System for Mobile Communications systems [6], and the 72- to 90-MHz bandwidth measurements at 1.8 GHz processed with 18-MHz resolution [2], there were no simultaneous comparative measurements in the frequency-division duplex (FDD) bands of 3G mobile radio systems. In an attempt to compare the FDD channels, single 15-MHz band measurements were used in [7]. Other reported FDD measurements were mainly concerned with the estimation of the angle of arrival and were performed with either 20-MHz bandwidth [8] or 5-MHz bandwidth [9]. Since the power in a resolved multipath component varies with frequency and bandwidth, and since 190 MHz separates the two FDD channels of 3G systems, it is important to simultaneously obtain measurements over the two bands.

To fully characterize the 3G FDD channels, the single-frequency sounder reported in [1] was upgraded to a dual-band sounder, which simultaneously transmits and receives at 1945 and 2135 MHz with 60-MHz bandwidth [10]. This paper presents the results of time delay dispersion measurements obtained with the sounder over the entire two 60-MHz UMTS bands. These measurements were performed in the dense urban environment of Manchester city center using both a trolley

Manuscript received August 2, 2001; revised October 1, 2004, February 21, 2006, August 25, 2006, November 30, 2006, and December 17, 2006. This work was supported by the Academic Development and Research Committee of the University of Manchester Institute of Science and Technology (UMIST). The review of this paper was coordinated by Prof. A. Abdi.

S. Salous was with the Department of Electronic and Electrical Engineering, University of Manchester Institute of Science and Technology, M60 1QD Manchester, U.K. She is now with the School of Engineering, Durham University, DH1 3LE Durham, U.K. (e-mail: sana.salous@durham.ac.uk).

H. Gokalp was with the University of Manchester Institute of Science and Technology, M60 1QD Manchester, U.K. She is now with the Department of Electrical Engineering and Electronics, Ondokuz Mayıs University, Samsun 55139, Turkey (e-mail: hkokalp@omu.edu.tr).

Color versions of one or more of the figures in this paper are available online at <http://ieeexplore.ieee.org>.

Digital Object Identifier 10.1109/TVT.2007.900495

and a van, which give characteristic data of typical pedestrian and vehicular mobile radio users. Nine different routes of up to 1.77-km transmit–receive distances were covered with the trolley, and a 4.1-km route was covered in the van. A total of 58 388 impulse responses were collected at 581 local areas: 56 locations collected in the van and 525 locations in the trolley measurements.

In this paper, the measurement system is briefly described, followed by a description of the measurement environment and the data processing. Medium-scale and large-scale results for the root-mean-square (rms) delay spread and the width of the profile are presented for the 5- and 60-MHz frequency resolutions. The distance and path loss dependency of the channel parameters are also studied and compared with previously reported studies. A model that relates the rms delay spread to distance and excess path loss is fitted to the measured data. The trolley data were primarily used in the analysis as the number of locations surveyed in the van was limited, and the receive antenna height was different from that used in the trolley.

II. MEASUREMENTS

A. Measurement System

Details of the dual-band channel sounder can be found in [10] and [11]. Briefly stated, the sounder employs a state-of-the-art digital chirp technique, which provides full programmability of the waveform parameters such as bandwidth, sweep repetition frequency (SRF), time delay window, carrier frequency, and Doppler resolution. The time delay resolution provided by the chirp technique is ideally inversely proportional to the swept bandwidth, and the unambiguous Doppler coverage is equal to $\pm\text{SRF}/2$. The sounder employs heterodyne detection, which enables the processing of data either over the whole bandwidth or subdividing it into sections to study the frequency dependence of the channel [2], [12]. For example, in this paper, the 60-MHz samples are divided into 12 sections to obtain the 5-MHz channel characteristics for wideband CDMA systems.

Sounder performance was verified from various back-to-back tests, including the ambiguity function to determine the resolution of the sounder in both time delay and Doppler shift, and the two-tone test to verify its linearity [11]. In this paper, the 5-MHz power delay profile (PDP) as a function of frequency over the two bands is presented in Fig. 1 to show that all the frequency sections have identical resolution, and the amplitude variations across each 60-MHz band are less than 1 dB.

The transmit and receive antennas are vertically polarized omnidirectional with 7- and 3-dB gains, respectively. The effective radiated power is 34 dBm. The measurements were simultaneously conducted at 1945 and 2135 MHz with 60-MHz bandwidths and with either 100- or 250-Hz SRF giving unambiguous Doppler ranges of ± 50 or ± 125 Hz, respectively. This corresponds to maximum relative speeds of 27 and 67.5 km/h, which are adequate to cover speeds in a high-density traffic environment. The unambiguous time delay window depends on the low-pass filter bandwidth, transmitted bandwidth, and SRF. For the present measurements, the time delay windows were 16.66, 27.5, and 41.66 μs .

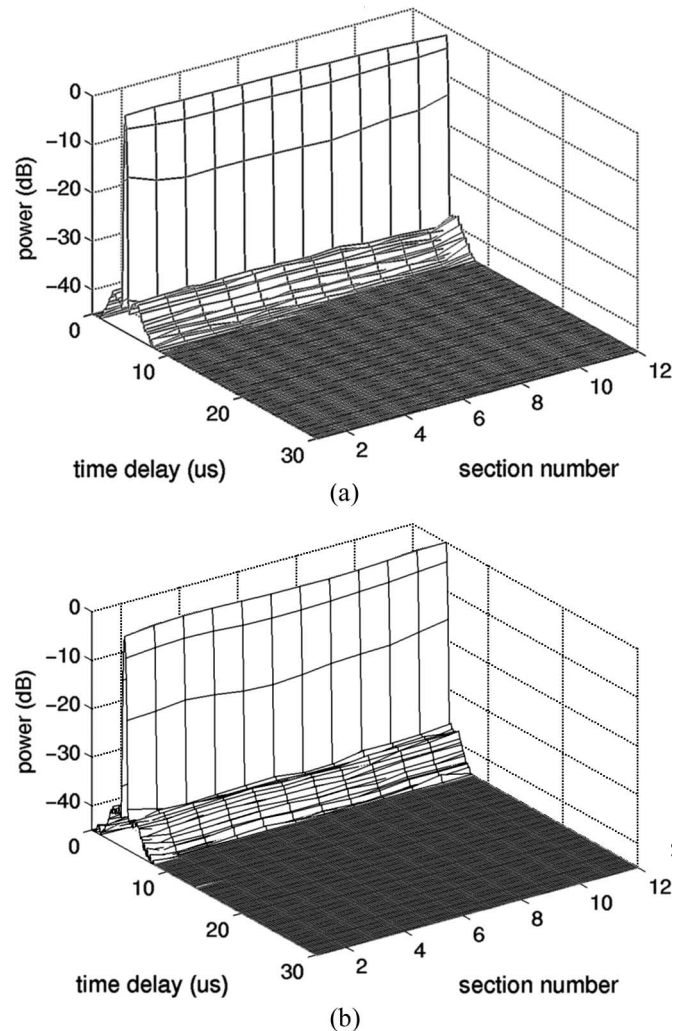


Fig. 1. Sounder performance as a function of frequency (a) uplink and (b) downlink.

B. Measurement Environment

Measurements were performed in the dense urban environment of Manchester city center in areas with high user density such as train stations, shopping areas, tunnels, and both narrow and wide streets. Various types of street orientations (radial, oblique, and circumferential) were covered. The city center mainly consists of seven- to ten-story buildings and a few 15- to 20-story buildings. The terrain and building profiles can be considered to be representative of many large European city centers, as can be seen in Fig. 2(a).

The transmit antenna was located 46 m above street level, and the receive antenna was 1.75 m above ground for the trolley and 2.5 m for the van. The map in Fig. 2(b) shows the measurement area. Due to the scale of the map, only six of the trolley routes (routes 1–3 and 6–8) are indicated. Channel data were acquired for the duration of 0.5–1 s, i.e., collecting each run consisting of 50–250 consecutive impulse responses, at each local area. The distance between local areas was about 20–40 m. The speed of the receiver was 30–60 km/h for the van and 1.5–3 m/s for the trolley measurements. Due to the movement of vehicles in the traffic, some of the measurements were taken while the receiver

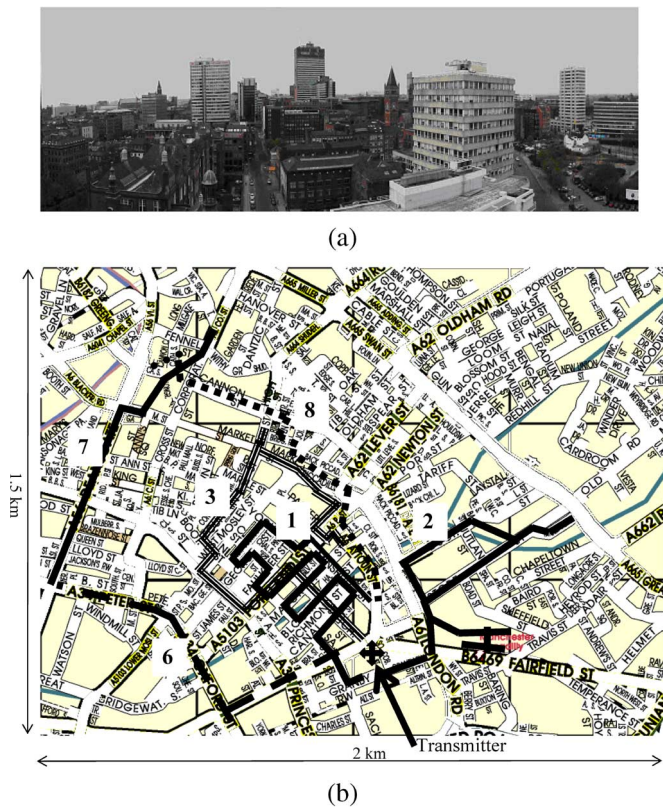


Fig. 2. (a) Measurement environment of the Manchester city center. (b) Map of the Manchester city center indicating some of the routes (grid line separation is 500 m).

was stationary. A record of the measurement location was kept during the field trials, and the range from the transmitter was subsequently calculated from scaled maps.

C. Processing of Data

The data were processed to obtain the time-variant impulse response for each run using the fast Fourier transform algorithm. Each PDP was then obtained by averaging the instantaneous PDPs for each local area. Due to the variations in receiver speed, these profiles represent either temporal averages (receiver stationary) or spatial averages (receiver moving). PDPs obtained from both types of averaging exhibited differences between uplink and downlink, where the temporal profiles showed finer and denser multipath components, and the spatial profiles were smoother [10]. The data were examined for the type of averaging by estimating the average Doppler for each 0.5- to 1-s run. The percentage of locations with Doppler shift was about 28%.

In spatial averaging, it is usual to average a number of instantaneous PDPs over tens of wavelengths. It is, however, necessary to consider the distance traveled by the mobile in relation to the time delay resolution of the sounder. For example, in the measurements reported by Cox [13] and Bajwa and Parsons [14], an average PDP was obtained over 5–30 and 5 m, respectively, where the corresponding resolutions of the sounders were 30 m. It is therefore appropriate to define the duration (or distance) over which an average delay profile is

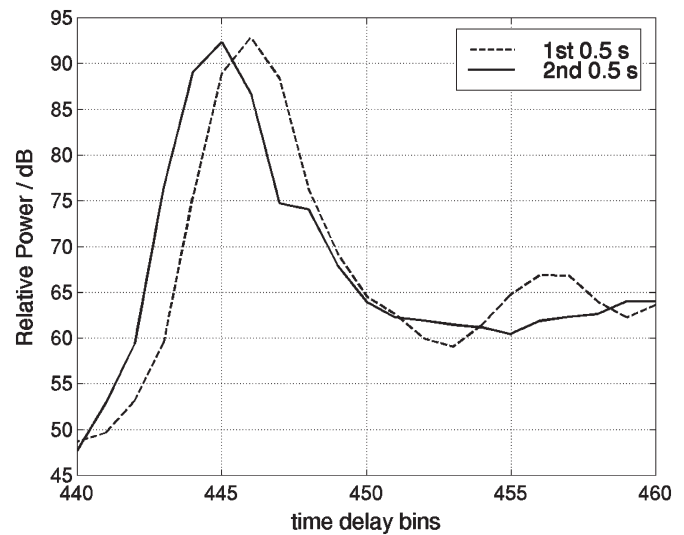


Fig. 3. PDPs showing the movement of the peak over 1-s measurement with the solid line showing the average over the first 0.5 s and the dashed line for the second 0.5 s.

obtained as the interval during which the multipath components do not move by more than half a delay bin. This can be related to the maximum observed Doppler shift. For example, for a 60-MHz bandwidth, the ideal range resolution is equal to 5 m. For 1 s of integration time, this limits the maximum Doppler shift to 33.3 Hz. For higher Doppler shifts, the time interval for averaging should be a fraction of a second, as shown in Fig. 3 for a measurement with 70-Hz Doppler shift. The figure shows the movement of the peak from one time delay bin to another over 1 s due to the high Doppler shift. This results in smearing of the delay profile, where the same multipath component is detected in several range bins and affects the overall estimate of the received power and rms delay spread. For the trolley data, the highest detected Doppler shift was on the order of 35 Hz, which is close to the above limit. The maximum Doppler shift experienced in the van measurements was 80 Hz. In this paper, the time averages were obtained over 0.5–1 s, which correspond to spatial distances between 0.75 and 12 m (3–80 wavelengths). Therefore, the observed small-scale differences between the two frequency bands detected in this paper can be attributed to the variations of the relative phase with frequency of the multipath components, which are not resolved within the time delay bin. Time averages of over 1 s were also reported in the study carried out by Seidel *et al.* [15].

The PDPs were obtained for each band either with 60-MHz resolution or with 5-MHz resolution, as shown in Fig. 4, for a measurement obtained while the van was on the move, which corresponds to a spatial average over 7 m. Both the 60-MHz and the 5-MHz PDPs show differences between uplink and downlink for both bandwidths despite the spatial averaging.

Occasionally, in-band interference, which was assumed to be due to predeployment field trials, is detected in the measurements, as seen in Fig. 5(a) and (b) for two different sweeps collected within 870 ms. The effect of interference in a chirp system has been previously studied by Shearman and Unsal [17], who have shown that narrowband interference raises the noise floor of the compressed chirp signal, hence reducing the

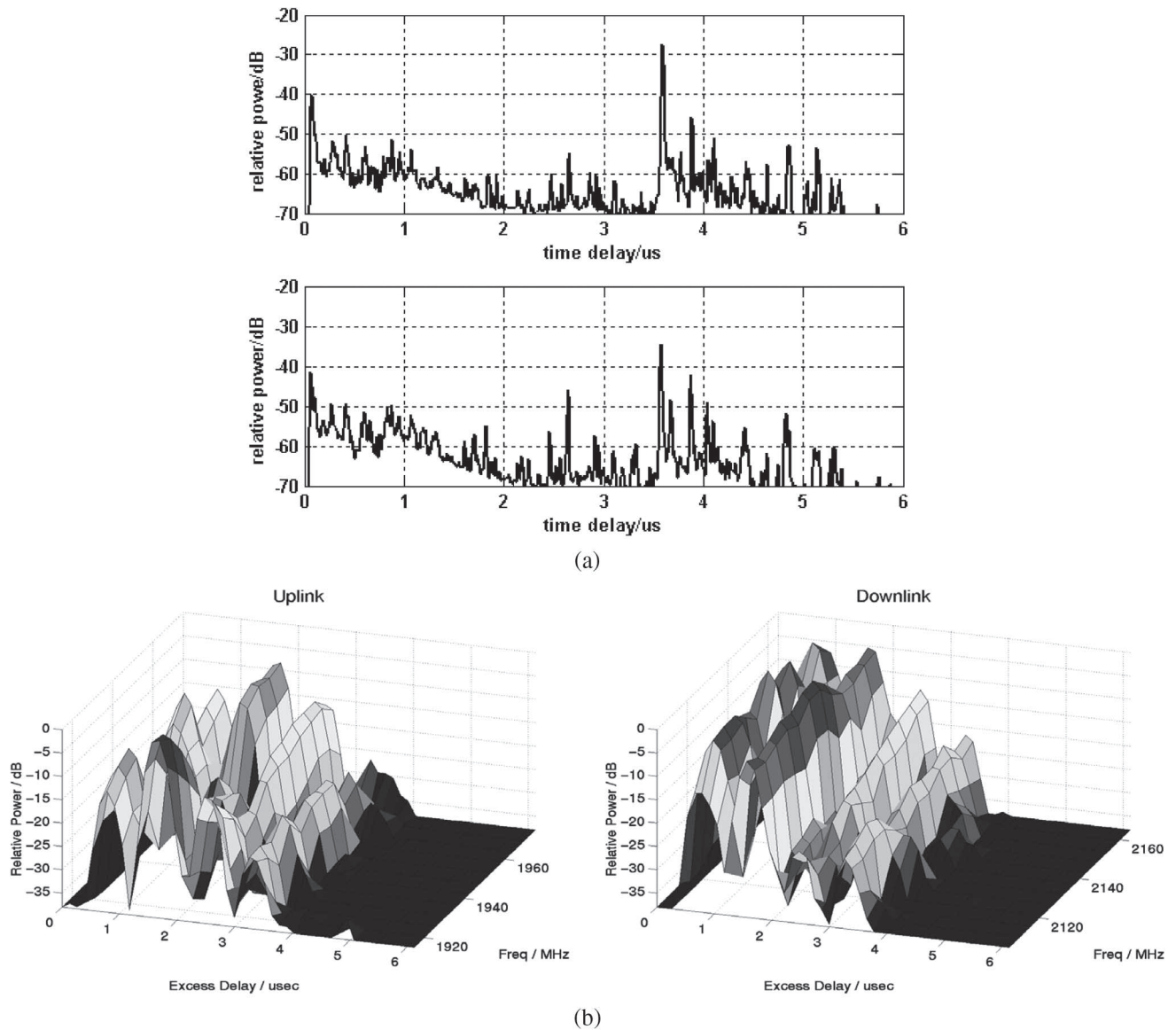


Fig. 4. PDP obtained from spatial averaging. (a) 60-MHz bandwidth with top figure for uplink and the lower figure for the downlink. (b) 5-MHz resolution over the 12 sections for (left) uplink and (right) downlink.

signal-to-noise ratio (SNR), as shown in Fig. 5(c), for two 5-MHz frequency sections. Due to the higher processing gain obtained with the 60-MHz bandwidth, the effect of interference is more pronounced with the 5-MHz sections. Enhancement of the SNR can be achieved either by clipping the interference or by choosing interference free sweeps [2], [11] to determine the PDP, as seen in Fig. 5(d) for the same frequency sections of Fig. 5(c).

To verify the spatial averaging distance for the present data, 30 files obtained from vehicular measurements were processed to obtain PDPs averaged over a different number of sweeps equal to 5, 10, 25, and 50 sweeps (20, 40, 100, and 250 ms) for both 60- and 5-MHz resolutions. This gives 5 to 50 PDPs in 1 s, which corresponds to different spatial averages depending on the vehicle's speed. The profiles were then used to estimate the rms delay spread, and the number of runs was subsequently entered into the tables in [16] to determine the

stationary distance for averaging. It was found that for 30- to 80-Hz Doppler shifts, the spatial averaging distance should not exceed 3 m with a minimum averaging distance of four to six wavelengths, i.e., 60–90 cm for the 60-MHz resolution, whereas for the 5-MHz resolution, the stationary distance could be in excess of the distance traveled in the 1-s interval. This confirms the previous statement regarding the relation between Doppler shift and resolution bandwidth. Each PDP was verified for a minimum of 25-dB SNR threshold. When any of the resulting profiles for any frequency section for either band did not satisfy the SNR criterion, the run was eliminated from the overall cumulative distribution for all sections for both links to ensure the same number of points for each section. The profiles were subsequently used to extract small-scale channel parameters such as average delay, rms delay spread, path loss, and the 15-dB width of the profile down from the peak (time between the first and the last time a threshold level is crossed).

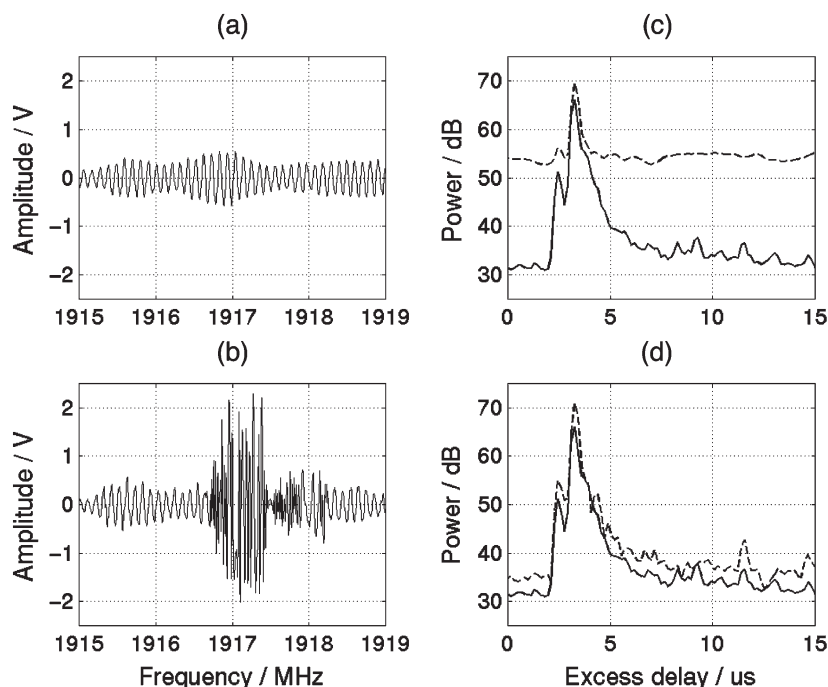


Fig. 5. Two sweeps separated by 850 ms with (a) no interference and (b) with interference. PDP for two 5-MHz sections (c) without interference clipping and (d) with interference clipping.

The small-scale channel parameters were combined to obtain either medium-scale characterization, i.e., for each route as shown in Fig. 6(a)–(d), or large-scale characterization by combining the data from all the routes. The characterization includes cumulative distribution functions (cdfs) for each frequency band separately either with 60-MHz resolution or with 5-MHz resolution, and probability distribution histograms of the difference between the uplink and downlink parameters on a local area basis for all the routes for both 60- and 5-MHz resolutions.

To study the effect of transmit–receive distance (range) and path loss on the measured channel parameters, data from all the trolley routes were grouped into three subgroups. The three range groups correspond to 500 m for the first two groups and 770 m for the third group. The three path loss groups correspond to 78–98, 98–118, and 118–138 dB. In addition, scatter plots of rms delay spread as a function of distance, path loss, and excess path loss were produced.

III. MEDIUM-SCALE AND LARGE-SCALE CHARACTERIZATIONS

In this section, the distributions of channel parameters for some of the routes are discussed for both 60- and 5-MHz resolutions.

A. Route Variability (Medium Scale)

The PDPs for each route as a function of local area were concatenated, as shown in Fig. 6, for both uplink and downlink for routes one and eight of the trolley measurements (medium-scale area). The profiles are normalized each with respect to its own peak and show the dependency of PDP on frequency

and location. Figs. 6 and 7 demonstrate that the extent of delay spread is a function of distance from the transmitter, street width, surrounding environment, and the route orientation with respect to the transmitter. For example, route one [Fig. 6(a)] covers narrow streets within the 500-m radius of the transmitter with 50% of the locations being along radial streets. The building heights along the route vary between five and seven stories. Route eight [Fig. 2(b)] covered the heart of the city center, including an open garden area and a shopping square. The covered streets were either circumferential or oblique with only 35% of the locations within 500 m from the transmitter and 11% between 1000 and 1100 m. The profiles acquired in the shopping square had a number of peaks and exhibited differences between the two 60-MHz bands. Fig. 7(b) and (d) also shows that an increase in path loss in excess of 120 dB from location 40 corresponded to an increase in rms delay spread. In these areas, the direct path was heavily shadowed, and the receiver was on circumferential streets at ranges greater than 700 m away from the transmitter and had a direct view of a number of 15- to 20-story buildings and buildings with metallic sidewalls.

The cdfs for the rms delay spread of these two routes, which represent minimum spread and relatively high delay spread, are shown in Fig. 8(a) for 60-MHz resolution and in Fig. 8(c) for one of the 5-MHz frequency sections. Two observations can be made: 1) The channel parameters are a function of the analysis bandwidth; and 2) the frequency dependence of the channel parameters is a function of the route orientation. For example, for route one, the channel parameters for both resolution bandwidths are similar for both uplink and downlink, whereas for route eight, considerable frequency differences are observed.

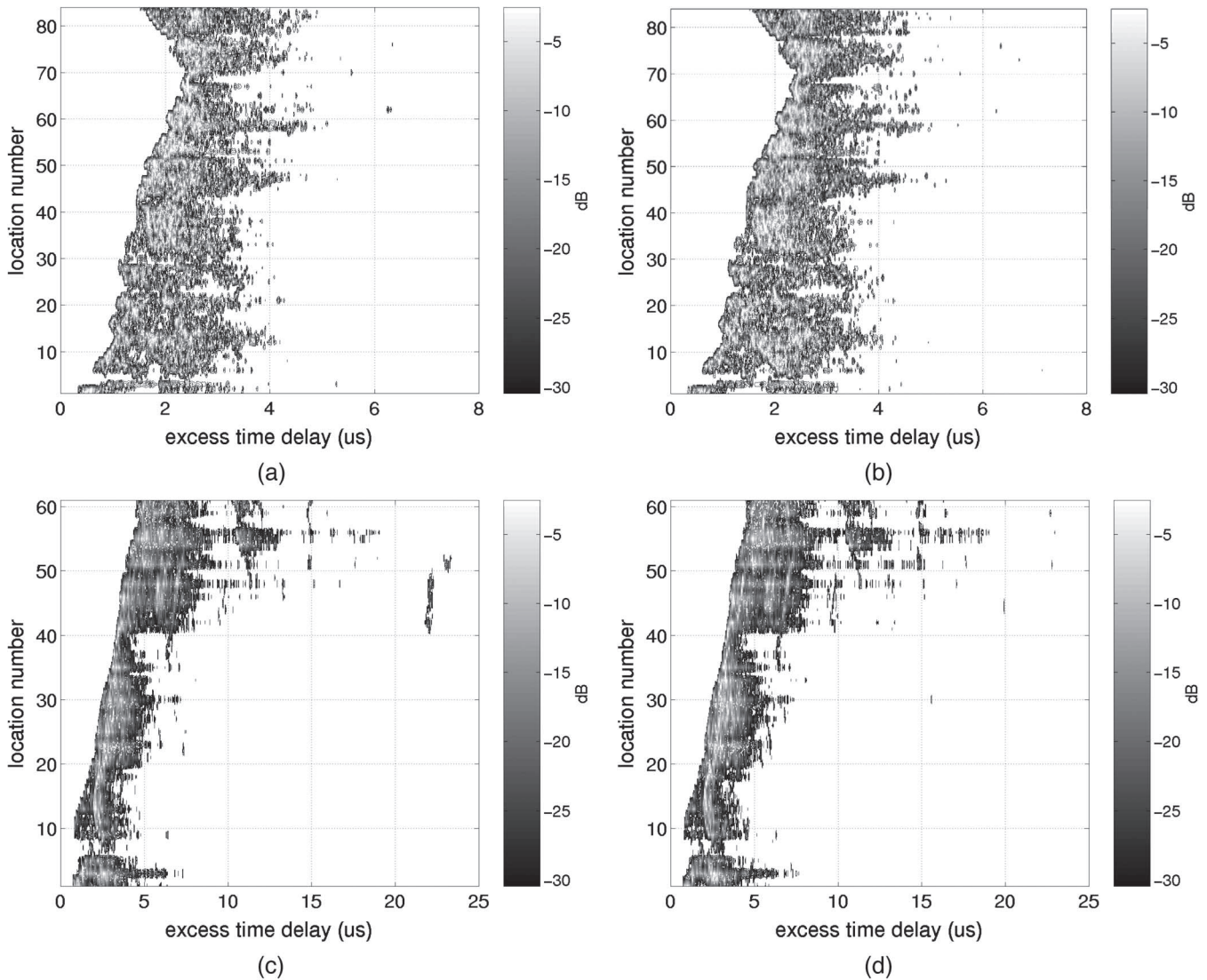


Fig. 6. PDP as a function of location for (a) route one uplink, (b) route one downlink, (c) route eight uplink, and (d) route eight downlink.

The variability between the different routes is assessed from the 90% values scaled from the cdf for each route for both 60- and 5-MHz resolution bandwidths. Fig. 9 displays the 90% values for the rms delay spread obtained with the 60-MHz resolution for the (solid line) uplink and (dashed line) downlink for the ten routes, where routes one to nine represent trolley routes, and route ten represents the van route. For visual clarity, note that in the figure, the downlink lines have been shifted to the right by a quarter of a number. Also shown in the figure is the corresponding 90% rms delay spread range of values over the twelve 5-MHz sections for both (circles) uplink and (stars) downlink. The figure shows the route variability between the two 60-MHz bands and also between the 5-MHz sections across the FDD bands. Large variations are seen to occur between the FDD bands for each user, and these can be significantly different from those experienced by another user operating on a different section of the spectrum.

Comparing the results for the two resolution bandwidths in shadowed routes (i.e., routes three, seven, eight, and ten), the values for the rms delay spread from the 5-MHz resolution are

considerably varied and tend to be larger than the corresponding values obtained with 60 MHz for either link. This indicates that the 60-MHz results cannot be directly used to indicate the 5-MHz dispersion along shadowed routes but can be considered more applicable to routes with low path loss values, i.e., both radial and narrow streets. The differences between the two bandwidths on shadowed locations are due to frequency-selective fading effects, which are more pronounced when the line of sight is heavily attenuated. Route nine was mainly along radial streets and, hence, experienced small dispersion.

Comparing the 60-MHz values, the largest differences for the 90% rms values were detected along routes eight and ten (van), and had values equal to 0.6 and 0.3 μs , respectively. An important parameter in the design of equalizers and RAKE receivers is the width of the profile. The largest 15-dB width difference between the two links was detected along route seven and was on the order of 8.3 μs for the 60-MHz resolution and 16 μs for the eighth frequency section with 5-MHz resolution.

The percentage route variability of the channel parameters was calculated from the ratio of the standard deviation to the

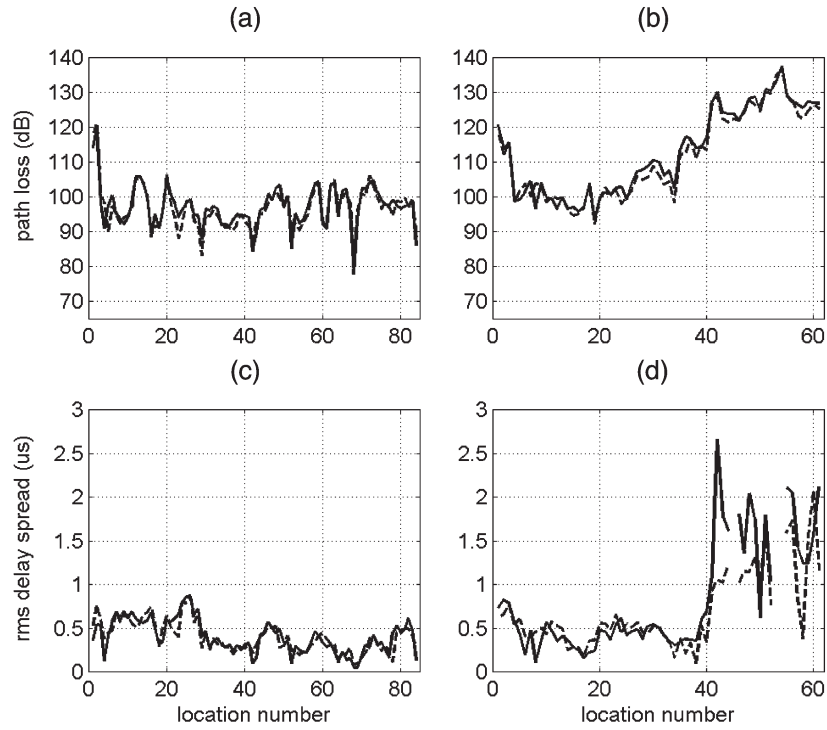


Fig. 7. Path loss as a function of location for (a) route one and (b) route eight. RMS delay spread as a function of location for (a) route one and (d) route eight. Solid line is uplink, and dashed line is downlink.

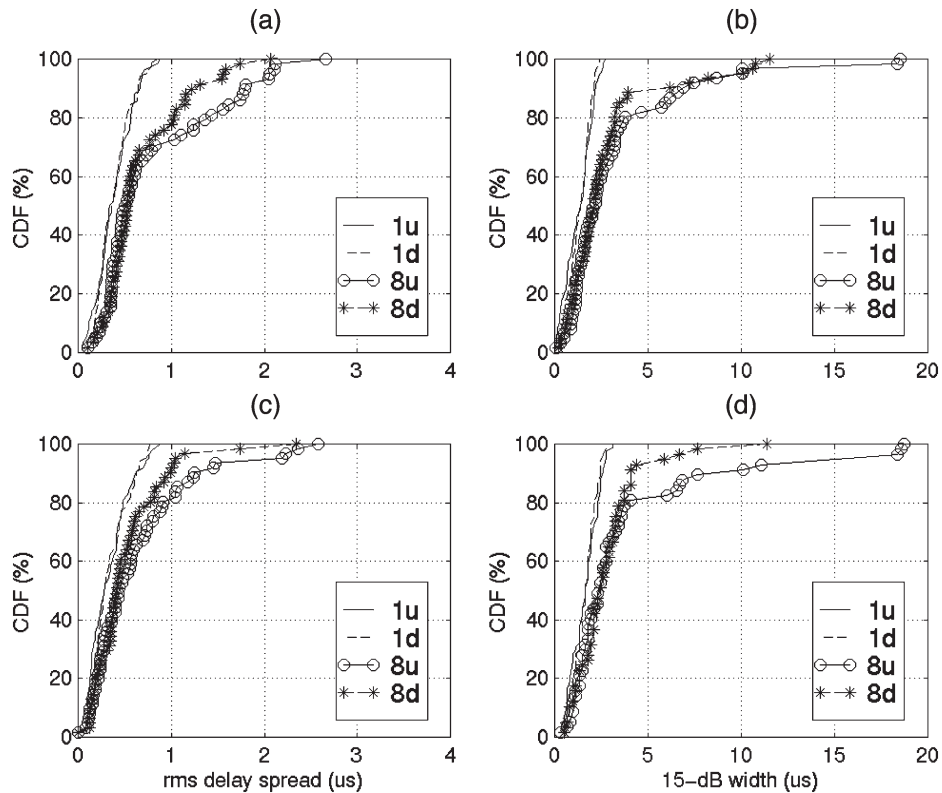


Fig. 8. CDFs of rms delay spread and 15-dB widths for routes one and eight (a) and (b) with 60-MHz resolution, (c) and (d) one 5-MHz section. 1u: route one uplink, 1d: route one downlink, 8u: route eight uplink, and 8d: route eight downlink.

mean for the 60-MHz resolution. For the 90% rms delay spread, the mean and percentage variabilities were equal to 1.1 μs and 50.7%, and 1.0 μs and 40.1%, for uplink and downlink,

respectively. These figures indicate that although the mean values for the two links are of similar order, the variability about the mean is quite high.

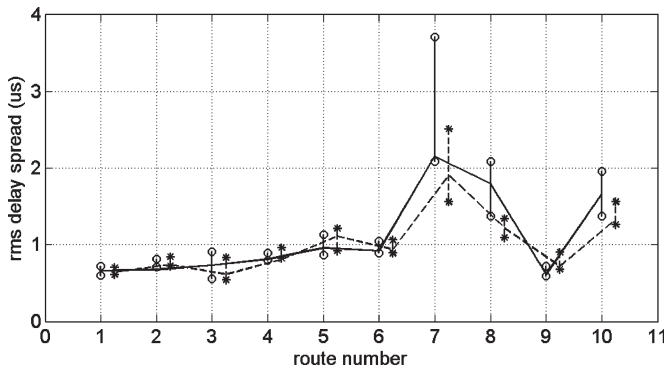


Fig. 9. Ninety percent of cdf of rms delay spread as a function of route number. Solid line with circles: uplink with 5-MHz resolution; solid line with star: downlink with 5-MHz resolution; solid line: uplink with 60-MHz resolution; and dashed line: downlink with 60-MHz resolution.

B. Large-Scale Characterization

Large-scale characterization is achieved in two ways. First, small-scale parameters were pooled from all the data to generate a single cdf (large scale) for each band, as shown in Fig. 10(a) and (b) for the rms delay spread and the 15-dB width of the profile for the 60-MHz bandwidth. The figure shows that, in general, the values for the two links are similar. This is due to the environment around the transmitter location, which is mainly characterized by radial streets and small streets. The locations, which exhibited shadow fading and were in sight of high-rise buildings, constituted only a small percentage of the measured locations and, hence, only affected the maximum values of the cdf.

Second, since the measurements at the two frequency bands were performed simultaneously, histograms of the difference at each location were computed as shown in Fig. 11(a) for the rms delay spread and Fig. 11(b) for the 15-dB width of the profiles obtained with 60-MHz resolution. The figures show that the difference values appear to be slightly biased to the left, i.e., the downlink experiences more spread than the uplink. For the 15-dB width, this bias was up to $2 \mu\text{s}$, and for values greater than $2 \mu\text{s}$, the bias was to the right. It was found that both the rms delay spread values and the 15-dB width values were higher for the downlink band for 55% of the time.

The highest detected difference for the 15-dB width from the histograms in Fig. 11 was on the order of $15.6 \mu\text{s}$ in comparison to the $8 \mu\text{s}$ obtained from the all-route cdf. This shows that while having a larger pool of data might reduce the bias in the histograms, the differences between the two links in certain locations can still be considerably higher than can be deduced from the cdf.

Fig. 12 shows similar histograms for two of the 5-MHz sections for the rms delay spread and the 15-dB width of the profiles. To assess the extent of variations as a function of frequency and bandwidth, the statistics for the percentage of locations for which the difference in the rms delay spread between the two links was greater by 100–500 ns in 100-ns steps were scaled for both 60- and 5-MHz resolutions. Also, values for the 15-dB width for which the difference between the two links was greater than 0.5, 1–3, and $5 \mu\text{s}$ were scaled.

For the 5-MHz sections, an average was obtained, and the results for the rms delay spread and 15-dB width are shown in Tables I and II, respectively. The tables show that higher differences can be detected with the 5-MHz bandwidth than with the 60-MHz bandwidth.

C. Distance and Path Loss Dependency of Time Dispersion

Distance and path loss dependence of the rms delay spread are studied using the trolley data only as few data points were collected with the van, and these were measured at a different antenna height. Regression analysis is applied to the data and a model, which takes into account both distance and excess path loss.

Also, the data were pooled into three groups according to two criteria, i.e., distance (range) and path loss. The first, second, and third range groups were for transmit–receive distances of 10–500, 500–1000, and 1000–1770 m, respectively (few data points were collected beyond 1770 m). The numbers of observations in each distance group were 262, 175, and 88, respectively. The data were also grouped according to path loss with groups from 78–98, 98–118, and 118–138 dB. The numbers of measurement locations in path loss group one, two, and three were 145, 298, and 82, respectively, for 60-MHz resolution. The cdf for the rms delay spread and the 15-dB width for 60-MHz resolution are shown in Fig. 13(a) and (b) for range and Fig. 13(c) and (d) for path loss, and Table III contains a summary of the 90% values and the median values of the cdf for both frequency resolutions. The 5-MHz range of values is shown in parenthesis. Generally, the channel parameters are observed to increase for both 5- and 60-MHz resolutions with distance and path loss, which is similar to the model proposed in [18]. The explanation offered in [18] for distance dependence was related to the attenuation experienced by the direct path and local scatterers as the receiver moves further away from the transmitter.

Table III shows a significant sudden increase in channel parameters for the third group regardless of distance or path loss. Also, significant differences are observed across the 12 frequency sections and between the FDD band parameters primarily for the third group. These variations can be attributed to the shadowing of the direct path, which causes the contribution from echoes with larger excess time delays to be detected, such as those from high-rise buildings, thus increasing the value of rms delay spread. This also enhances the differences between the different frequency bands as the different multipath components fade differently with frequency, as can be seen in Fig. 4. Generally, fewer variations across the different frequency bands and between sections were observed in the presence of the line-of-sight component. The effect of shadowing can also be observed in Fig. 7 and from the scatter plot of rms delay spread versus distance in Fig. 14, which show small multipath dispersion at large distances when the receiver moved to a less shadowed area.

To verify some of the assumptions proposed by Greenstein *et al.* [18], the rms delay spread data were fitted to lognormal, Nakagami, Rayleigh, Rice, Suzuki, and Weibull distributions, and the Kolmogorov–Smirnov goodness-of-fit was

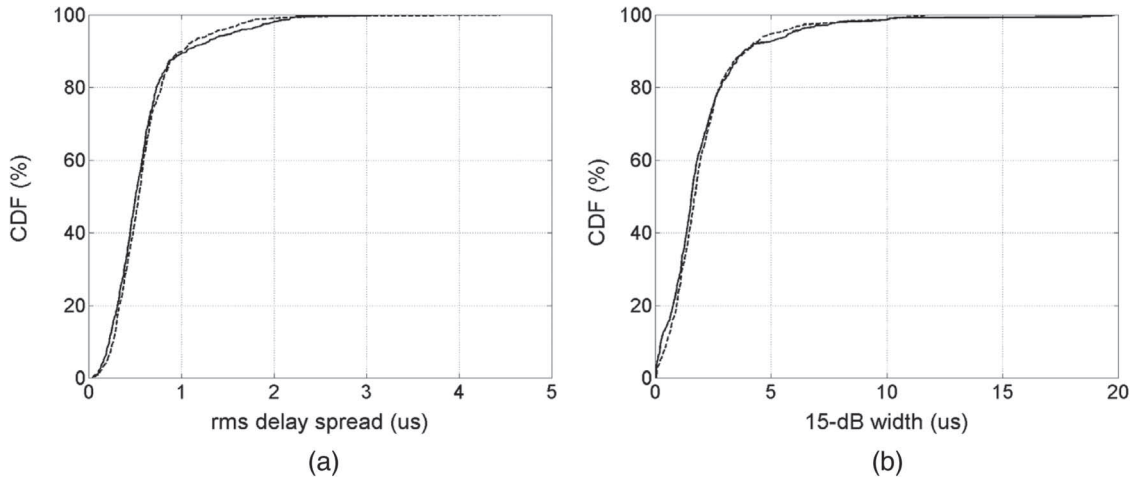


Fig. 10. All-route cdf for 60-MHz resolution. (a) RMS delay spread. (b) 15-dB widths.

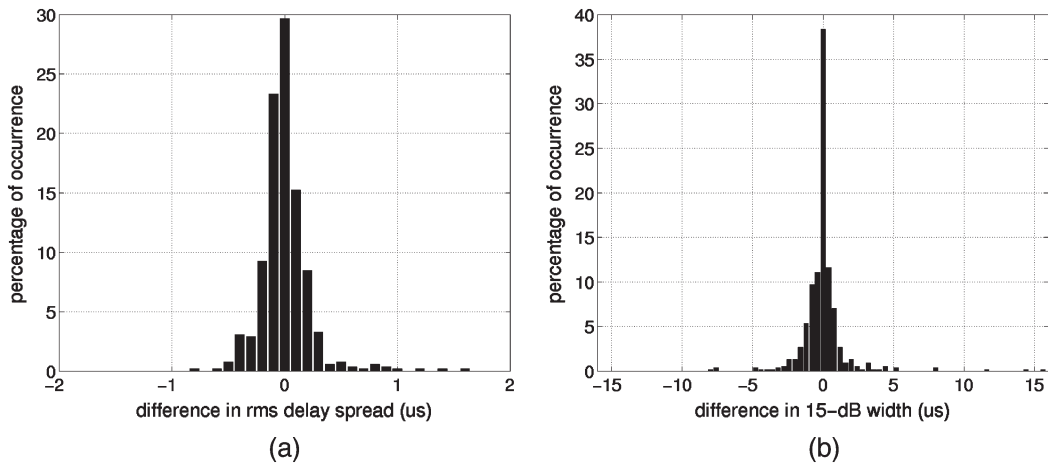


Fig. 11. Histograms of the difference between uplink and downlink on a local area basis with 60-MHz (a) RMS delay spread and (b) 15-dB width.

used to indicate the suitability of the distribution. It was found that the lognormal distribution had the best fit for the rms delay spread from all the locations as suggested by Greenstein *et al.* [18].

In an attempt to study the correlation between delay spread, distance, and path loss, Greenstein *et al.* [18] proposed a model based on scaled values of cdf from a number of published papers. The model assumes that the delay spread at a particular distance follows a lognormal distribution. The model gives relationships for the median delay spread of an area (τ_{med}) to distance and the median delay spread at 1 km (T_1). The relationship is distance raised to a value between 0.5 and 1 for terrain ranging from urban to mountainous. The relevant equation for urban areas is given by

$$\tau_{med}(\text{area}) = 0.76T_1d_{max}^{0.5} \tag{1}$$

where d_{max} is the maximum radius of the area of measurements.

An attempt was made to apply (1) to our measurements. Since the model assumes uniform distribution, and since most

of our measurements in the 900- to 1100-m range were in shadowed locations, (1) was rewritten in the form of

$$\frac{\tau_{2(\text{med})}}{\tau_{1(\text{med})}} = \left(\frac{d_2}{d_1}\right)^\epsilon \tag{2}$$

and used to estimate the value of ϵ using the measured values of rms delay spread at 300 m (150 points), 500 m (105 points), and 700 m (60 points) by taking data points in 200-m intervals. To avoid the bias due to the varying number of samples in each group, the same number of data points, i.e., 60 points, was used to estimate the median.

For these distances, the median rms delay spread was 0.47, 0.42, and 0.49 μs , which gives a value for ϵ equal to 0.56 for maximum distances of 600 and 800 m, and 0.04 for maximum distances of 400 and 800 m. While the first value is close to the proposed 0.5 factor, the second value is significantly smaller. This indicates a weak dependence of the rms delay spread on distance as can be seen from the median values for the three distances where the median for the first group is higher than for the second group. This can also be confirmed from the median

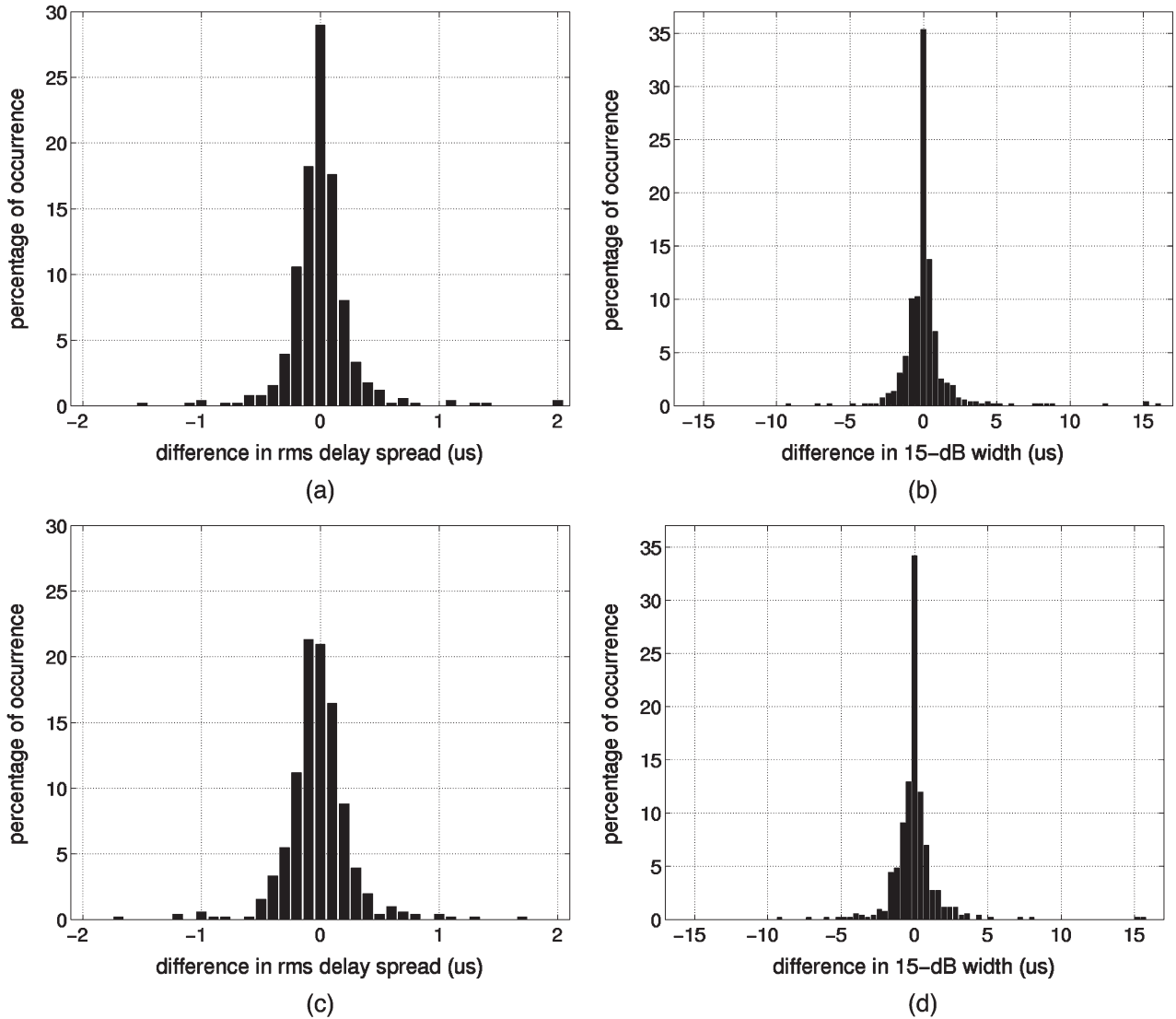


Fig. 12. Histograms of the difference between uplink and downlink on a local area basis for two 5-MHz sections (sections two and seven). (a) and (c) rms delay spread and (b) and (d) 15-dB width.

TABLE I
RMS DELAY SPREAD VALUES DEDUCED FROM HISTOGRAMS

25-dB rms delay spread	Percentage of locations where differences greater than				
	0.1 μ s	0.2 μ s	0.3 μ s	0.4 μ s	0.5 μ s
60-MHz	50.09	19.08	10.79	6.17	3.85
5-MHz	55.1	28.34	15.3	8.6	5.5

TABLE II
FIFTEEN-dB WIDTH VALUES DEDUCED FROM HISTOGRAMS

15-dB width	Percentage of locations where differences greater than				
	0.5 μ s	1 μ s	2 μ s	3 μ s	5 μ s
60-MHz	41.02	22.12	8.96	5.16	1.91
5-MHz	44.3	25.1	9.6	4.8	1.94

of the measurements obtained with the van that was equal to 0.54 μ s for the uplink despite the fact that the maximum distance extended up to 4.1 km, which far exceeds the 1.77-km distance of the trolley measurements. This also gives a small value of ϵ , which is about 0.1.

Devasirvatham [19] also attempted to relate distance and rms delay spread and found inconsistencies between different sets of measurements and also found that the rms delay spread occasionally decreased for long distances. This was also observed in this paper, where the smallest rms delay spread of 15 ns was detected at 2.5 km away from the transmitter. It is interesting, however, that Greenstein *et al.* [18] used the scatter plot of rms delay spread versus received power of Devasirvatham [19] to prove their distance relationship, where ϵ is deduced to be equal to 0.48.

In [19], a different fit between the logarithm of the rms delay spread and the received power (normalized with respect to 0.3 m) was given, which was also found to not be suitable. This could be attributed to the environment, where in [19] the measurements were conducted in small cities and covered short distances. In addition, most buildings were three stories or lower, and the transmit and receive antenna heights were 1.8 and 9.1 m, respectively. Due to the low antenna heights, propagation is governed by the scatterers in the vicinity of the mobile. Although low antenna heights mean higher path loss

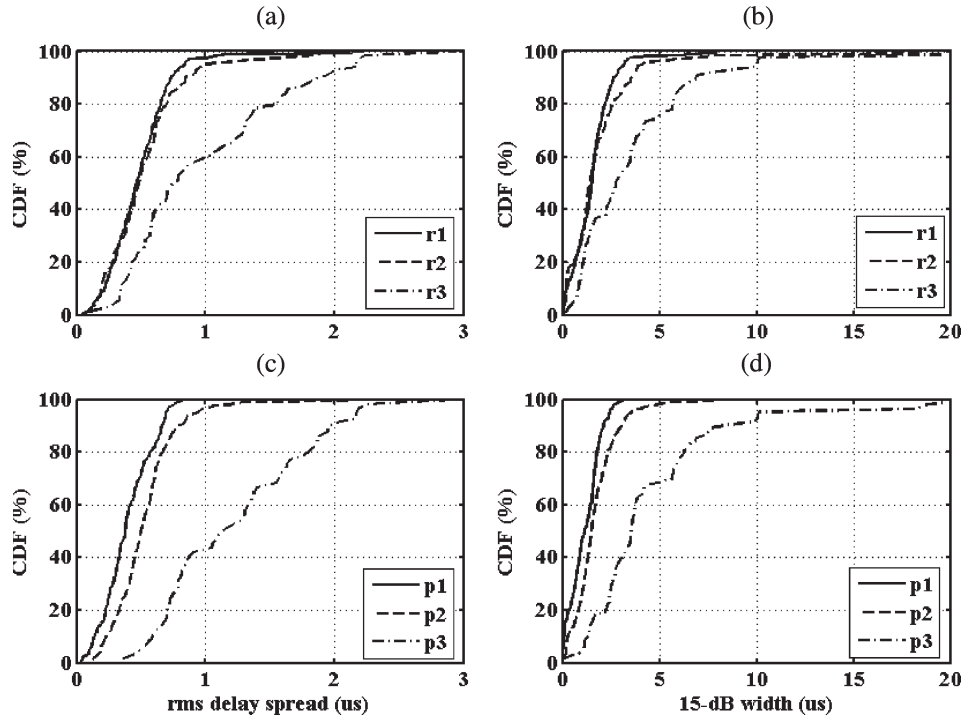


Fig. 13. CDFs for the three distance groups (r1: 10–500 m, r2: 500–1000 m, and r3: 1000–1770 m) and for the three path loss groups (p1: 78–98 dB, p2: 98–118 dB, and p3: 118–138 dB). (a) and (c) RMS delay spread. (b) and (d) 15-dB width.

TABLE III

(a) 90% VALUE RMS DELAY SPREAD AND 15-dB WIDTH OF PROFILES FOR DIFFERENT DISTANCE GROUPS AND PATH LOSS GROUPS FOR 60 MHz.
 (b) MEDIAN-VALUE RMS DELAY SPREAD AND 15-dB WIDTH OF PROFILES FOR DIFFERENT DISTANCE GROUPS AND PATH LOSS GROUPS FOR 60 MHz

Groups	Link	25-dB rms delay spread μ s, 90%		15-dB width μ s, 90%	
		Range	Path loss	Range	Path loss
Distance: up to 500 m	uplink	0.72, (0.7-0.8)	0.67,(0.65-0.72)	2.63, (2.77-3.1)	2.13, (2.2-2.5)
Path loss: 78-98 dB	downlink	0.74, (0.74-0.83)	0.67, (0.67-0.74)	2.72,(2.77-3.26)	2.4, (2.3-2.75)
Distance: 500 m-1 km	uplink	0.94, (0.84-1)	0.79, (0.87-1.1)	3.6, (3.58-4.23)	3.1, (3.6-3.9)
Path loss: 98-118 dB	downlink	0.91, (0.82-0.97)	0.82, (0.9-1.22)	3.34, (3.1-3.9)	3.1, (3.6-4.6)
Distance: 1-1.77 km	uplink	1.92, (1.82-2.18)	1.97, (1.5-1.95)	6.87, (6.35-10.1)	8.7, (6.5-10.5)
Path loss: 118-138 dB	downlink	1.55, (1.57-2.14)	1.73, (1.5-1.95)	7.1, (6.18-10.25)	8.3, (6.5-10.5)

The values in parenthesis represent the range of values for the 5-MHz 12 frequency sections.

(a)

Groups	Link	25-dB rms delay spread μ s, median		15-dB width μ s, median	
		Range	Path loss	Range	Path loss
Distance: up to 500 m	uplink	0.46, (0.43-0.51)	0.38, (0.31-0.39)	1.52, (1.55-1.82)	1.15, (1.1-1.6)
Path loss: 78-98 dB	downlink	0.51, (0.47-0.51)	0.46, (0.36-0.44)	1.66, (1.7-1.82)	1.42, (1.3-1.6)
Distance: 500 m-1 km	uplink	0.48, (0.45-0.52)	0.5, (0.46-0.48)	1.41, (1.5-1.8)	1.51, (1.7-1.82)
Path loss: 98-118 dB	downlink	0.45, (0.46-0.56)	0.53, (0.45-0.48)	1.48, (1.45-1.8)	1.74, (1.6-1.8)
Distance: 1-1.8 km	uplink	0.75, (0.49-0.62)	1.1, (0.9-1.1)	2.65, (2.1-3.0)	3.52, (3.25-3.9)
Path loss:118-138 dB	downlink	0.77, (0.49-0.6)	1.16, (0.9-1.0)	2.75, (1.8-2.9)	3.56, (2.9-3.8)

The values in parenthesis represent the range of values for the 5-MHz 12 frequency sections.

(b)

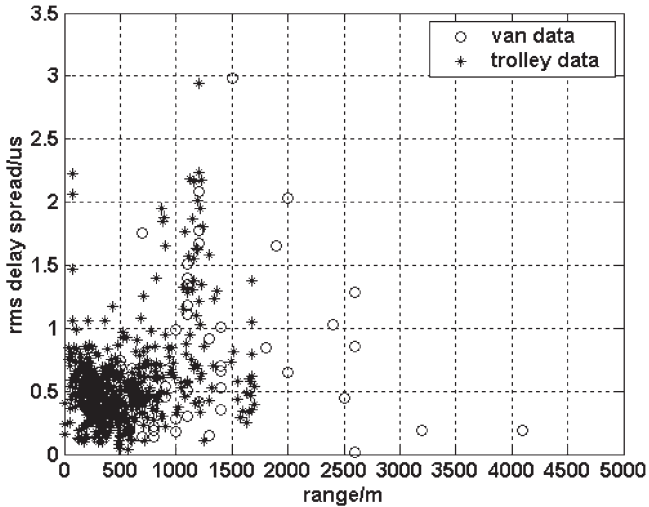


Fig. 14. Scatter plot of rms delay spread versus transmit-receive range in meters. + is the trolley data, and o is the van data.

values, which could result in high rms delay spread values, as the antenna heights are decreased, the antennas become visible to fewer scattering objects at greater distances. This gives smaller rms delay spread values.

For the present measurements, a suitable fit relating the rms delay spread in nanoseconds to the path loss in decibels for the two links

$$\log_e \tau_{\text{rms}} \text{ (in nanoseconds)} = 2.43 + 0.0358 P_L \text{ (in decibels)} \quad (3.a)$$

$$\log_e \tau_{\text{rms}} \text{ (in nanoseconds)} = 2.92 + 0.0309 P_L \text{ (in decibels)} \quad (3.b)$$

[(3.a) uplink and (3.b) downlink] was found from all the trolley measurements for the distance between 110 and 1.77 km, where the measured range of path loss was between 78 and 138 dB. To isolate the interdependence between path loss and distance, as in [20], a scatter plot between rms delay spread and excess path loss EP_L was computed using first regression analysis to find the path loss coefficients and subsequently by taking the difference between the measured path loss and the regression fit. The path loss coefficients were found to be 2.56 and 2.42 for both uplink and downlink, respectively. Equation (3) can then be rewritten in terms of the excess path loss as

$$\begin{aligned} \log_e \tau_{\text{rms}} \text{ (in nanoseconds)} &= 0.0358 EP_L \text{ (in decibels)} \\ &\quad + 0.916 \log_{10} d \text{ (in meters)} \\ &\quad + 3.73 \end{aligned} \quad (4.a)$$

$$\begin{aligned} \log_e \tau_{\text{rms}} \text{ (in nanoseconds)} &= 0.0309 EP_L \text{ (in decibels)} \\ &\quad + 0.748 \log_{10} d \text{ (in meters)} \\ &\quad + 4.14. \end{aligned} \quad (4.b)$$

The model of (4) shows a linear relationship with excess path loss but a logarithmic relationship with distance. For the range of variations in EP_L (see Fig. 15) and d , the delay spread variations are more affected by the increase of excess path loss

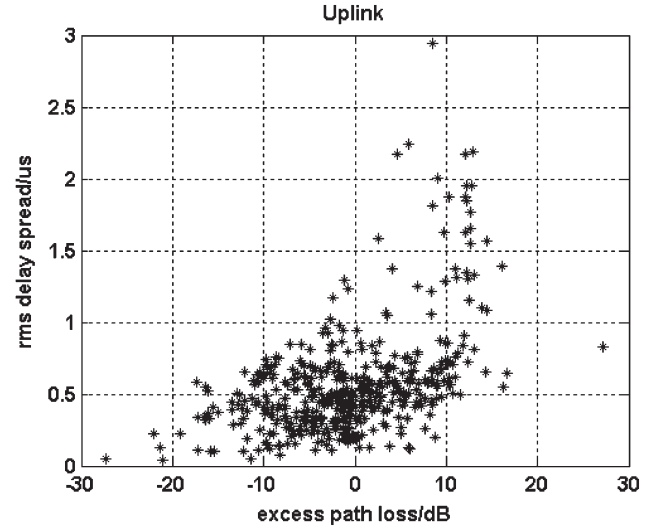


Fig. 15. Scatter plot of rms delay spread versus excess path loss for trolley data.

than with distance. This result might be of relevance to cell planning since more dispersion leads to more complex system design.

The scatter plot of rms delay spread versus excess path loss for the uplink shown in Fig. 15 also indicates an exponential relationship between rms delay spread and excess path loss. Thus, regression analysis was performed using the natural logarithm of delay spread in nanoseconds, excess path loss EP_L in decibels, and distance in meters. The results were then compared with (4), and the maximum difference between the two fits was found to be 80 ns.

In [21], an overbound exponential fit between rms delay spread and path loss was given, where the path loss was normalized with respect to 1 m. The model given in [21] was found to be not suitable for our measurements. This could be attributed to the difference in antenna height, where the measurements reported in [21] were conducted with transmit antenna heights between 3.7 and 13.3 m, whereas the measurements reported here were conducted with a transmit antenna height of 46 m.

Finally, the correlation coefficients between rms delay spread and distance, and rms delay spread and excess path loss, were computed. The correlations with distance for the uplink and downlink values were found to be equal to 0.39 and 0.4, respectively. The corresponding values for the excess path loss correlations were 0.51 and 0.49 for the respective links. Although neither correlation coefficient is high, the correlation between distance and rms delay spread is slightly lower than between excess path loss and delay spread.

IV. CONCLUSION

Time dispersion results of simultaneous measurements across the 60-MHz FDD UMTS bands in a dense urban environment have been presented. PDPs representative mainly of temporal averages (72%) have been used in the analysis. The data have been studied for frequency and bandwidth dependence, and the dependency of rms delay spread on path loss and distance has been compared with published models.

The frequency and bandwidth dependence were found to be related to shadowing. In the presence of a dominant line-of-sight component, the other multipath components and, in particular, far away echoes make a smaller contribution to the resultant received signal; hence, time dispersion parameters are independent of frequency and bandwidth. In contrast, in a shadowed location, a large number of relatively comparable strength components are detected in addition to echoes from distant high-rise buildings. As the frequency is varied, the relative phase between these components in a particular time delay bin varies with frequency, which gives rise to differences in the time dispersion parameters. Similarly, as the resolution bandwidth of analysis is varied, the total number of unresolved multipath components in a particular time delay bin varies, which results in larger differences in delay spread parameters.

Pooling of the large-scale data using the commonly used cdf and histograms of the difference on a local area basis showed that much greater differences can be detected between the FDD bands at certain locations than can be inferred from cdf.

The rms delay spread was found to fit a lognormal distribution, as proposed by Greenstein *et al.* [18], but when the measured data were fitted to the distance relationship proposed by Greenstein *et al.* [18], a discrepancy was found. Other relationships proposed by Devasirvatham [19] and Feuerstein [21] between rms delay spread and path loss were also found to not be suitable for the measurements in this paper.

To include the effects of both distance and excess path loss, a regression fit between rms delay and excess path loss and distance was derived from the measurements. The correlation coefficients between rms delay spread and excess path loss were found to be 0.5 for a path loss coefficient of about 2.5. This value is smaller than the 0.75 correlation reported by Greenstein *et al.* [18] for a path loss coefficient of 3.58. The correlation coefficient between distance and time dispersion was found to be 0.4.

ACKNOWLEDGMENT

The authors would like to thank the assistance of the research students V. Hinostrroza, P. Filippidis, M. Abd-Allah, and R. Lewenz in the field trials and the anonymous referees, whose comments helped enhance the quality of this paper.

REFERENCES

- [1] S. Salous, N. Nikandrou, and N. F. Bajj, "Digital techniques for mobile radio chirp sounders," *Proc. Inst. Elect. Eng.—Commun.*, vol. 145, no. 3, pp. 191–196, Jun. 1998.
- [2] S. Salous, "Measurements of multipath delay statistics over 72–90 MHz bandwidth at 1.8 GHz in two European cities using a chirp sounder," *Radio Sci.*, vol. 34, no. 4, pp. 797–816, Jul.–Aug. 1999.
- [3] D. M. J. Devasirvatham, M. J. Krain, and D. A. Rappaport, "Radio propagation measurements at 850 MHz, 1.7 GHz and 4 GHz inside two dissimilar office buildings," *Electron. Lett.*, vol. 26, no. 7, pp. 445–447, Mar. 1990.
- [4] P. L. Nobles and F. Halsall, "Delay spread and received power measurements within a building at 2 GHz, 5 GHz and 17 GHz," in *Proc. 10th ICAP*, Apr. 14–17, 1997, vol. 2, pp. 2.319–2.324.
- [5] G. L. Turin, F. D. Clapp, T. L. Johnstone, S. B. Fine, and D. Lavry, "A statistical model for urban multipath propagation," *IEEE Trans. Veh. Technol.*, vol. VT-21, no. 1, pp. 1–9, Feb. 1972.
- [6] J.-C. Bic and P. Pajusco, "Results on frequency cross correlation from wideband measurements at 1.8 GHz," France Telecom CENT, Belfort, France, COST Rep. 231 TD(95), 1995. 6 p.
- [7] M. Beach, B. Allen, and P. Karlsson, "Spatial decorrelation of frequency division duplex links," *Electron. Lett.*, vol. 36, no. 22, pp. 1884–1885, Oct. 26, 2000.
- [8] M. Beach, P. Eneroth, S. E. Foo, J. Johansson, P. Karlsson, B. Lindmark, and D. McNamara, "Description of a frequency division duplex measurement trial in the UTRA frequency band in urban environment," Bologna, Italy, COST 273 TD (01) 028, 2001.
- [9] K. Hugl, K. Kalliola, and J. K. Laurila, "Spatial reciprocity of uplink and downlink radio channels in FDD systems," Helsinki, Finland, COST 273, TD (02) 066, 2002.
- [10] S. Salous and H. Gokalp, "Dual frequency sounder for UMTS frequency division duplex channels," *Proc. Inst. Elect. Eng.—Commun.*, vol. 149, no. 2, pp. 117–122, Apr. 2002.
- [11] H. Gokalp, "Characterisation of UMTS FDD channels," Ph.D. dissertation, Univ. Manchester Inst. Sci. Technol., Manchester, U.K., 2001.
- [12] S. Salous and H. Gokalp, "Propagation measurements in FDD UMTS bands," in *Proc. ICAP*, Apr. 2001, pp. 137–141.
- [13] D. C. Cox, "910 MHz urban mobile radio propagation: Multipath characteristics in New York City," *IEEE Trans. Commun.*, vol. COM-21, no. 11, pp. 1188–1194, Nov. 1973.
- [14] A. S. Bajwa and J. D. Parsons, "Large area characterization of urban UHF multipath propagation and its relevance to the performance bound of mobile radio systems," *Proc. Inst. Elect. Eng. F*, vol. 132, no. 2, pp. 99–106, Apr. 1985.
- [15] S. Y. Seidel, T. S. Rappaport, S. Jain, M. L. Lord, and R. Singh, "Path loss, scattering, and multipath delay statistics in four European cities for digital cellular and microcellular radiotelephone," *IEEE Trans. Veh. Technol.*, vol. 40, no. 4, pp. 721–730, Nov. 1991.
- [16] J. S. Bendat and A. G. Peirsol, *Measurements and Analysis of Random Data*. Hoboken, NJ: Wiley, 1966, p. 170.
- [17] E. D. R. Shearman and R. R. Unsal, "Compatibility of high frequency radar remote sensing with communications," in *Proc. Int. Conf. Radio Spectrum Conservation Tech.*, IEE, London, U.K., Jul. 1980, pp. 103–107.
- [18] L. J. Greenstein, V. Erceg, Y. S. Yeh, and M. V. Clark, "A new path-gain/delay-spread propagation model for digital cellular channels," *IEEE Trans. Veh. Technol.*, vol. 46, no. 2, pp. 477–485, May 1997.
- [19] D. M. J. Devasirvatham, "Radio propagation studies in a small city for universal portable communications," in *Proc. 38th IEEE Veh. Technol. Conf.*, 1988, pp. 100–104.
- [20] E. S. Sousa *et al.*, "Delay spread measurements for the digital cellular channel in Toronto," *IEEE Trans. Veh. Technol.*, vol. 43, no. 3, pp. 837–849, Nov. 1994.
- [21] M. Feuerstein *et al.*, "Path loss, delay spread and outage models as functions of antenna height for microcellular system design," *IEEE Trans. Veh. Technol.*, vol. 43, no. 3, pp. 487–497, Aug. 1994.



Sana Salous (M'95) received the B.E.E. degree from the American University of Beirut, Lebanon, in 1978 and the M.Sc. and Ph.D. degrees from the University of Birmingham, Birmingham, U.K., in 1979 and 1984, respectively.

She was an Assistant Professor with Yarmouk University, Irbid, Jordan, until 1988 and a Research Associate with the University of Liverpool, Liverpool, U.K., until 1989, at which point, she took up a lecturer post with the Department of Electronic and Electrical Engineering, University of Manchester Institute of Science and Technology (UMIST), Manchester, U.K. She was promoted to Senior Lecturer in 2000 and Reader in 2003, at which point, she took up the Chair in Communications Engineering with the School of Engineering, Durham University, Durham, U.K. She is currently with Durham University.



Hulya Gokalp received the B.Sc. degree from the Middle East Technical University, Ankara, Turkey, in 1993, the M.Sc. degree from Brunel University, London, U.K., in 1997, and the Ph.D. degree from the University of Manchester Institute of Science and Technology (UMIST), Manchester, U.K., in 2001.

Since 2001, she has been a Lecturer with the Department of Electrical Engineering and Electronics, Ondokuz Mayıs University, Samsun, Turkey. Her research interests include radio channel propagation, signal processing, bandwidth-efficient modulation schemes, and wireless communication systems.